

Detecting and localizing anomalies on masonry towers from low-cost vibration monitoring

Paolo Borlenghi^a, Carmelo Gentile* and Antonella Saisi^b

Department of Architecture, Built environment and Construction engineering (ABC),
Politecnico di Milano, Piazza Leonardo da Vinci 32, 20133 Milan, Italy

(Received July 8, 2020, Revised November 11, 2020, Accepted November 21, 2020)

Abstract. The structural health of masonry towers can be monitored by installing few accelerometers (or seismometers) at the top of the building. This cost-effective setup provides continuous and reliable information on the natural frequencies of the structure and allows to detect the occurrence of structural anomalies; however, to move from anomaly detection to localization with such a simplified distribution of sensors, a calibrated numerical model is needed. The paper summarizes the development of a Structural Health Monitoring (SHM) procedure for the model-based damage assessment in masonry towers using frequency data. The proposed methodology involves the subsequent steps: (i) preliminary analysis including geometric survey and ambient vibration tests; (ii) FE modeling and updating based on the identified modal parameters; (iii) creation of a Damage Location Reference Matrix (DLRM) from numerically simulated damage scenarios; (iv) detection of the onset of damage from the analysis of the continuously collected vibration data, and (v) localization of the anomalies through the comparison between the experimentally identified variations of natural frequencies and the above-defined DLRM matrix. The proposed SHM methodology is exemplified on the ancient *Zuccaro* tower in Mantua, Italy. Pseudo-experimental monitoring data were generated and employed to assess the reliability of the developed algorithm in identifying the damage location. The results show a promise toward the practical applications of the proposed strategy for the early identification of damage in ancient towers.

Keywords: damage localization; masonry tower; model updating; historical constructions; structural health monitoring

1. Introduction

In the last decades, the assessment and preservation of ancient masonry towers have become a prominent research topic due to the intrinsic vulnerability of these structures. Most likely, the increasing attention on historic towers started after the sudden collapse of the Civic Tower of Pavia in 1989 (Binda *et al.* 1992), which was not considered at risk at that time. Consequently, several towers were investigated in the years ahead: the *Torrazzo* of Cremona (Binda *et al.* 2000), the St. Stefano bell-tower in Venice (Lionello *et al.* 2004), the bell-tower of Monza Cathedral (Gentile and Saisi 2007), the tower of the Provincial Administration Building in Bari (Diaferio *et al.* 2007), the Qutb Minar in Delhi (Peña *et al.* 2010). In the last few years, the number of studies increased considerably, focusing mainly on two aspects: seismic assessment (see, e.g., Bartoli *et al.* 2016, Valente and Milani 2016, Milani and Clementi 2019), and condition monitoring (Gentile *et al.* 2016, Azzara *et al.* 2018, Ubertini *et al.* 2018). In addition, a list of recent studies on ancient towers is reported in Diaferio *et al.* (2018).

In this context, Structural Health Monitoring (SHM) has become a valuable tool for the preservation of ancient towers and, in general, of monumental buildings (see, e.g., Lorenzoni *et al.* 2013, Potenza *et al.* 2015, Masciotta *et al.* 2016, Elyamani *et al.* 2017, Gentile *et al.* 2019a, Kita *et al.* 2019, Zonno *et al.* 2019). Among numerous SHM techniques, measuring the vibrations induced by operational loads – namely, vibration-based monitoring (VBM) – is of utmost interest due to its fully non-destructive nature and its minimum impact. The main advantages of VBM are: (i) the relatively limited number of sensors needed to capture the global dynamic behavior of a structure; (ii) the opportunity of performing the analysis with the structure fully operating; (iii) the possibility of correlating the extracted modal parameters with the onset of damage. In masonry towers, the cantilever-like dynamic behavior can be exploited to monitor the structural conditions with few sensors placed at the top of the building. This cost-effective measurement setup has demonstrated to provide continuous and reliable information on the natural frequencies of the structure (Ramos *et al.* 2013, Cantieni 2014, Gentile *et al.* 2016, Ubertini *et al.* 2018). However, two issues must be considered: (1) natural frequencies are highly affected by environmental effects, and (2) moving from detection to localization using only frequency data requires a theoretical model of the structure.

The possibility of correlating the changes in the identified modal parameters and the onset of damage has inspired numerous researchers over the years, creating the

*Corresponding author, Professor,
E-mail: carmelo.gentile@polimi.it

^a Ph.D. Student, E-mail: paolo.borlenghi@polimi.it

^b Associate Professor, E-mail: antonella.saisi@polimi.it

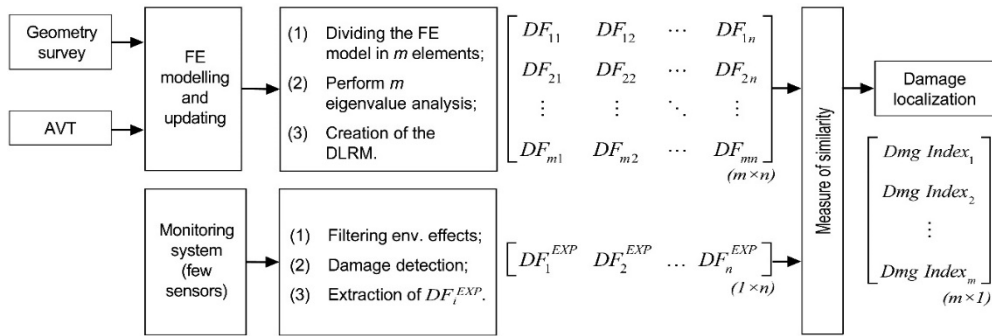


Fig. 1 Proposed damage identification scheme for masonry towers

research field of vibration-based damage identification (VBDI). The nature, location, and severity of damage can affect the modal parameters of the investigated structure differently, enabling the detection, localization, and quantification of the occurred anomaly. The first comprehensive review of VBDI methods was carried out at Los Alamos Laboratories in the mid-1990s (Doebling *et al.* 1998), reporting more than 100 studies. Recent investigations on masonry towers (Gentile *et al.* 2016, Ubertini *et al.* 2018) have demonstrated that the anomalous changes in frequency data can be distinguished by the common variations caused by environmental effects, using regression tools and novelty analysis. Among different regression techniques, Principal Component Analysis (PCA, Jolliffe 2002) has been widely applied to correlate frequency and environmental parameters (Yan *et al.* 2005, Bellino *et al.* 2010, Cabboi *et al.* 2017). Subsequently, statistical control tools, such as the multivariate control charts (Montgomery 1997), can be applied to the filtered data, detecting the occurrence of abnormal variations in the structural response.

Identifying the position of damage using only the observed changes in natural frequencies is clearly of interest, as frequency data are relatively simple to estimate. Nevertheless, this approach usually involves the development of a theoretical model of the structure. Recently, the issue of damage localization has been investigated in the context of SHM for masonry towers. Cabboi *et al.* (2017) proposed an approach using surrogate-based FE model updating. Once the fluctuations caused by environmental effects are removed using regression analysis, the FE model of the structure is updated each time a new observation is available and a new set of structural parameters is identified. Consequently, abnormal changes in structural parameters are detected and correlated with their location. On the other hand, the resolution in the localization is limited to the number of updating parameters that should be smaller than the number of experimental frequencies considered. Similarly, Venanzi *et al.* (2020) used a surrogate-based procedure involving mode shapes and natural frequencies to localize a slight change in the structural behavior identified from the continuous monitoring of the *Sciri* tower (Perugia, Italy). Subsequently, the localization was successfully validated using non-linear dynamic analysis and visual inspections. However, the resolution in the damage localization is still limited by the

number of updating parameters.

Within the framework of ancient masonry towers, the objective of the paper is to extend the capability of VBM systems, employing few sensors, towards a more effective damage localization. To this purpose, the cleaned frequency changes identified from continuous monitoring are compared to several damage scenarios computed with a calibrated numerical model. In other words, the proposed approach is based on the measure of similarity between the experimental frequency shifts and a damage sensitivity matrix, named Damage Localization Reference Matrix (DLRM). The FE model of the structure is employed to study how damage, in a specific location, affects the mutual variation between the natural frequencies.

The proposed methodology – summarized in Fig. 1 – involves the following steps: (i) preliminary analysis, including geometric survey and ambient vibration tests (AVTs); (ii) FE modeling and updating; (iii) creation of a Damage Location Reference Matrix (DLRM) from numerically simulated damage scenarios; (iv) detection of the onset of damage from dynamic monitoring; (v) localization of the anomalies through the comparison between the experimentally identified variation of natural frequencies and the DLRM matrix, containing information on the numerically simulated damage scenarios. Compared to previous studies using a sensitivity-based approach (see, e.g., Kim and Stubbs 2003, Messina *et al.* 1998), the present technique is not limited to academic examples or very simple structures, and can be applied to three-dimensional structures. Furthermore, for a single damage position, the use of a similarity measure guarantees that a correct indication of the damage location is provided with noisy data.

In the first part of the paper, the main ideas of the DLRM approach are presented by referring to an idealized masonry tower; subsequently, the proposed methodology is exemplified by referring to the real case of the *Zuccaro* tower in Mantua, Italy (Saisi *et al.* 2019, Gentile *et al.* 2019b). It is worth mentioning that the investigated building turns out to be especially interesting for the following reasons: (a) a quite large number of natural frequencies were identified using only four measuring channels; (b) the shape of the two upper modes suggested a warping distortion of the cross-section; (c) the installation of

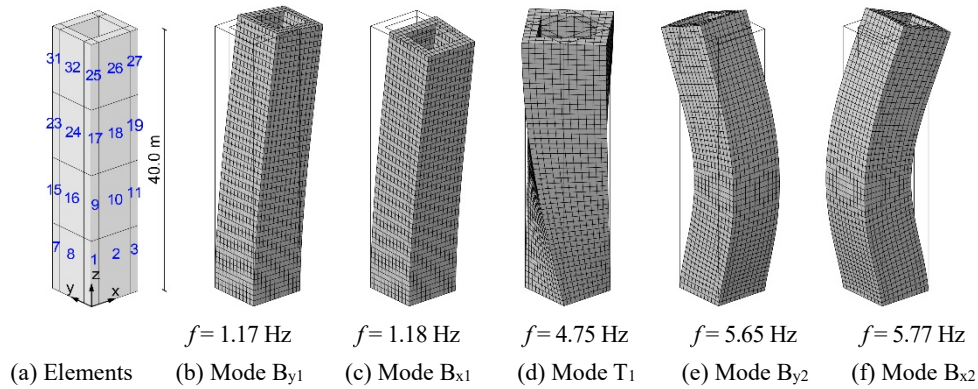


Fig. 2 Idealized tower divided into 32 elements and vibration modes used in the damage localization

a dynamic monitoring system on the tower has been already scheduled, with the support of the Cultural Heritage Superintendence of Mantua. After the calibration of a numerical model of the *Zuccaro* tower, pseudo-experimental monitoring data are generated from the updated model, and the reliability of the DLRM algorithm in identifying the damage location is demonstrated.

2. Damage identification methodology

The DLRM approach (Fig. 1) is developed to give information on the damage location using only the observed changes in natural frequencies.

To clarify the working principles of the proposed approach, the model of an idealized masonry tower is used. Fig. 2 shows the geometry adopted and the n vibration modes considered. As pointed out by different scholars (see, e.g., Cabboi *et al.* 2017, Ubertini *et al.* 2018, Standoli *et al.* 2020), five modes are often identified with Operational Modal Analysis in masonry towers: the first torsion mode (T) and four bending modes (B).

2.1 Initial steps

Firstly, the numerical model of the structure is developed and calibrated based on preliminary investigations, namely, geometric survey and ambient vibration testing. At the same time, a monitoring system with few sensors is installed on the structure, and the natural frequencies are identified and tracked by applying state-of-art techniques.

2.2 Analysis of monitoring data

The fluctuations caused by the environmental effects are removed using a PCA-based regression (Jolliffe 2002). For this purpose, the structure is analyzed during a reference period – usually referred to as training period – to study the seasonal effects induced by temperature and other external factors. Once the training period is completed, the occurrence of structural anomalies is investigated through the residual errors between predicted and identified frequency data (see, e.g., Cabboi *et al.* 2017).

Statistical tools, such as the control charts, are used to

detect the anomalous variations in the data. Control charts are graphical representations of the evolution over time of a certain process with designed control limits: an observation is considered abnormal when the control limit is exceeded. In SHM, the control limits are evaluated during the training period when the structure is assumed to be undamaged. The successful use of control charts in damage detection of ancient towers has been reported by Gentile *et al.* (2016) and Ubertini *et al.* (2018). In this paper, the Hotelling multivariate control chart based on the T^2 statistic (Hotelling 1947) is adopted.

The residual errors of the n frequencies – obtained from the PCA – are divided into subgroups composed by r elements. Let $x_i \in \mathfrak{R}^n$ the vector of the n averages of the i -th subgroup and $x^* \in \mathfrak{R}^n$ the vector of the averages of the residuals of the control group (training period). The statistical distance considered is defined as

$$T_i^2 = r \cdot (x_i - x^*)^T \cdot S^{-1} \cdot (x_i - x^*) \quad (1)$$

$$i = 1, 2, \dots, N/r$$

where r is the number of observations in each subgroup, $S \in \mathfrak{R}^{n \times n}$ is the covariance matrix of the control group, and N is the total number of observations.

Since the statistical distance in Eq. (1) is positive by definition, the Lower Control Limit (LCL) is taken equal to zero, whereas the Upper Control Limit (UCL) is defined as the T^2 value corresponding to a certain confidence level α during the training period.

Once an anomaly has been detected, the corresponding frequency shifts must be extracted. Since the residuals are affected by a certain variability, a mean value of H hours (e.g., 24 hours) should be defined for both the undamaged and the damaged state. The mean of the residuals in the undamaged state should be very close to zero, whereas the mean of the residuals in the damage state should correspond with the real frequency shifts. Consequently, a vector with n experimental frequency shifts is defined.

2.3 Creation of the DLRM

From the calibrated numerical model, a series of damage scenarios are simulated, and the consequent variations of natural frequencies are collected in a matrix called DLRM. Through a comparison of similarity between the frequency

variations in the DLRM and the ones given by the cleaned observations, it is possible to locate in which area the anomaly appears.

The DLRM contains the m percentage of variations of the n considered natural frequencies. The creation of the DLRM is performed as follows: (i) as shown in Fig. 2(a), the previously calibrated FE model is divided into m elements by differentiating corners and walls in plan, and floors in height; (ii) m eigenvalue analyses are performed reducing the elastic modulus of each element by a certain quantity (e.g., the 40%); (iii) the changes in the n natural frequencies are collected in an m -by- n matrix called DLRM.

It should be noticed that the number of elements m in which the tower is divided (Fig. 2(a)) is dependent on the geometry of the investigated building; on the other hand,

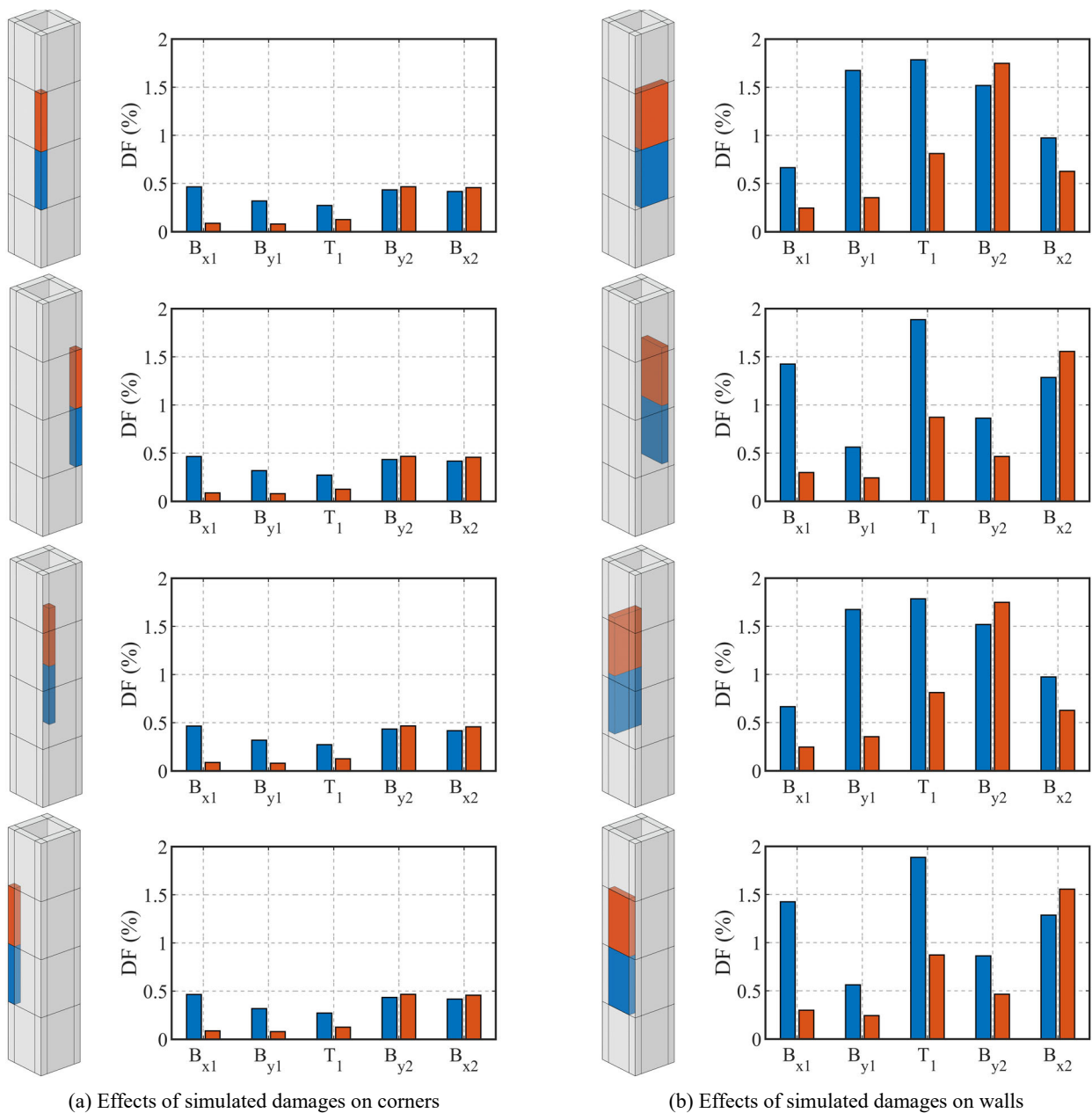
differentiating the 4 corners and the 4 load-bearing walls of each level can be considered as choice of general value.

The effects of the different simulated damages are described through the frequency discrepancy, defined as

$$DF_i = \frac{f_i^u - f_i^d}{f_i^u} \cdot 100 \quad (2)$$

where the i -th natural frequency before and after the damage occurrence is represented by f_i^u and f_i^d , respectively.

To give an example of how the location of damage affects the natural frequencies, Fig. 3 illustrates the comparison between the simulated damages of the idealized tower for the elements of two consecutive floors. The damages are obtained reducing the elastic modulus of each element by 30%.



(a) Effects of simulated damages on corners (b) Effects of simulated damages on walls
 Fig. 3 Comparison between the simulated Damage Scenarios (DSs) of the first and second floor in terms of frequency discrepancy (DF, Eq. (2))

From the analysis of this simplified application, it is possible to draw the following observations on the effectiveness of the localization procedure using the frequency variations: (i) the simulated damages belonging to different floors gives in all cases different pattern of frequency variations (Fig. 3); (ii) the simulated damages of the four corner elements belonging to the same level (bars with the same color in Figs. 3(a)-(b)) gives the same frequency variations; (iii) the simulated damages on the four wall elements belonging to the same floor (bars with the same color in Figs. 3(c)-(d)) gives the same frequency variations when aligned on the same direction.

2.4 Frequency-based damage localization

Once the onset of damage is detected, it is possible to

identify its location, analyzing the variation of natural frequencies. Comparing the observed frequency shifts with the m simulated damage scenarios, it is possible to locate the damage among the m elements previously identified. The Cosine Similarity is adopted to measure the similarity between the vector of the identified experimental frequency shifts (DS_{EXP}) and the m vectors of the simulated damage scenarios (DS_j)

$$\cos \theta_j = \frac{DS_j \cdot DS_{EXP}}{\|DS_j\| \cdot \|DS_{EXP}\|} \quad (3)$$

where θ_j is the j -th angle between the two vectors. In the present paper, the adopted Damage Index (DI) is expressed as follow

$$Damage\ Index_j = (\cos \theta_j)^2 \quad (4)$$

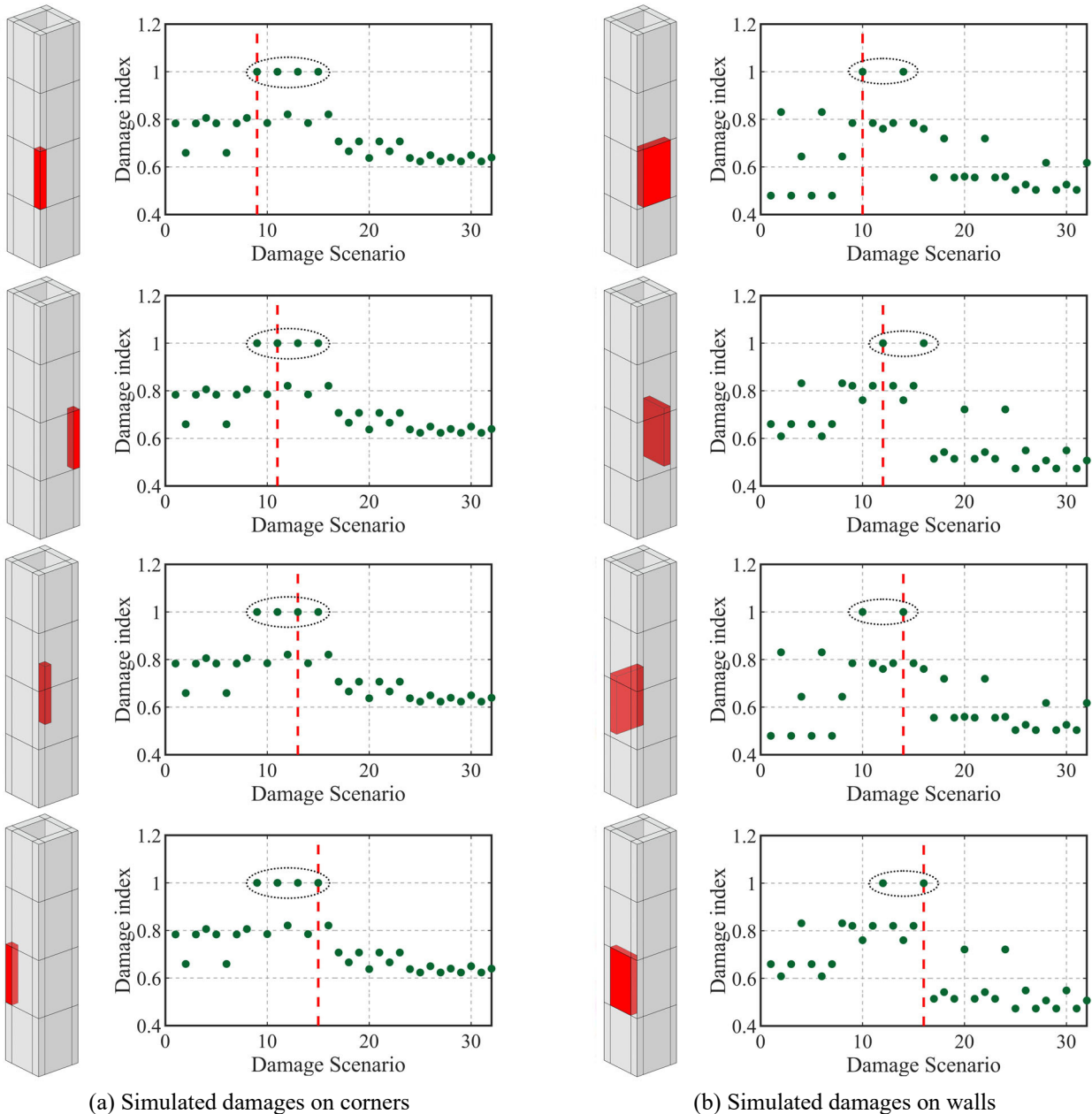


Fig. 4 Localization of 8 simulated damages obtained by decreasing the Young's modulus of first-floor walls and corners by 20% (the red dashed line represents the actual damage location)

where values close to 1 suggest a good correlation with the identified frequency shifts while values lower than 0.8 suggest a poor correlation. The m DI are then plotted together to better understand the results; consequently, the localization is performed considering the location associated with the higher DI (Fig. 4). Even if the localization should be driven by the higher DI values, the definition (4) suggests that a DI value higher than 0.90 should provide a reasonable threshold to be adopted in the localization.

In Fig. 4, the localization procedure is exemplified using the model of the idealized tower. Eight simulated frequency

shifts (DS_{EXP}) are computed reducing the elastic modulus of the eight elements of the first floor by the 20%. The different simulated DS_{EXP} are then compared with the j -th DS of the DLRM. The following observations can be drawn:

- as expected, it is not possible to distinguish between the DSs on corner elements belonging to the same floor;
- similarly, it is not possible to differentiate between the DSs on wall elements belonging to the same level and same direction.



(a) External views



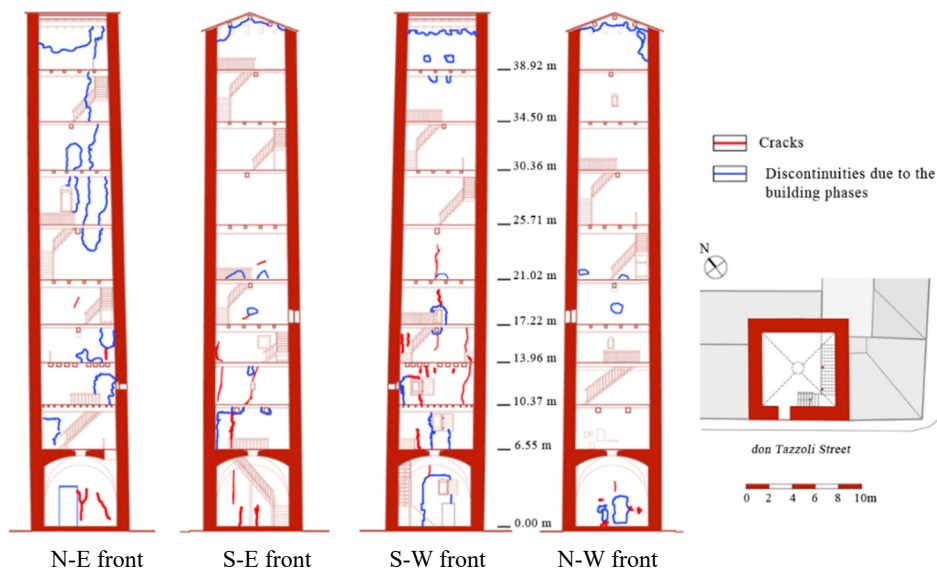
(b) Internal views on N-E front, ground floor



(c) Internal views on N-E front, second floor



(d) Internal views on N-E front, seventh floor



(e) Overall damage survey of the inner fronts

Fig. 5 The *Zuccaro* tower: external and internal views, and damage survey of the inner fronts

In conclusion, a numerical model of an idealized tower was employed to exemplify the application of the DLRM approach showing promising results. It should be noticed that increasing the number and the type (e.g., bending, torsion, or local) of vibration modes can substantially increase the effectiveness of the localization capability of the proposed approach.

3. The Zuccaro tower (Mantua, Italy)

The *Zuccaro* tower (Fig. 5), about 43 m high, is a defensive structure built in the Middle Ages (Saisi *et al.* 2019) in the historic town of Mantua. The first record regarding its existence dates back to 1143. The few and small openings and the tower location at the limits of the city Middle Ages fortifications suggest its original defensive role. As shown in Fig. 5(a), the tower is nowadays included in a building aggregate, surrounded on three-sides by low-rise constructions.

The structure has an approximate squared plan with the side equal to 8.5 m. The load-bearing walls are built in solid brick masonry with thickness ranging from 1.1 m at the base to 0.8 m at the top. A brick masonry cross vault is covering the ground floor, and a timber staircase is connecting the eight timber floors distributed along the height of the structure (Fig. 5(e)). It is worth mentioning that the roof and the timber floors were substituted after a fire occurred in 1979, and the related intervention, carried out in the 90s, involved the mortars injection in several areas.

Due to a large number of uncertainties regarding the evolution of the building and the effectiveness of strengthening interventions, an extensive investigation survey was recently carried out involving visual inspection and AVT. The results of the investigations are fully reported by Saisi *et al.* (2019) and Gentile *et al.* (2019b). The survey was aimed at providing details on the geometry of the structure, detecting critical areas and irregularities, and identifying the dynamic characteristics of the building (i.e., natural frequencies and mode shapes).

3.1 On-site inspections and documentary research

The results of on-site inspections of the tower inner fronts are summarized in Fig. 5(e). From the stratigraphic survey, the discontinuities caused by different building phases or local masonry reconstructions are identified. Furthermore, the on-site inspections highlighted the following aspects:

- Sharp discontinuities and deep cracks were found around the corner between the S-W and S-E walls starting from the base up to 17.22 m;
- Some deep and thick cracks were identified on the cross vault at the ground level;
- The presence of large areas with fragmentary and non-homogeneous masonry was identified starting from the height of 21.0 m on the N-E front (see Fig. 5(e));
- Extended dark areas resulting from the fire of 1979 were found in the inner walls.

Furthermore, the documentary research revealed the existence of numerous experimental analyses carried out in the early-1990s by ISMES (ISMES 1990). From the retrieved report, the average Young’s modulus identified from the double flat jack tests in the lower part of the tower was equal to 3.18 GPa.

3.2 Dynamic characteristics of the tower

Two series of AVTs (Gentile *et al.* 2019b) were conducted on the tower involving a different number of sensors. The first test (4 measuring channels) was performed between October 23rd and 24th, 2016, with the twofold objective of identifying the vibration modes of the structure and evaluating the effectiveness of a 4-sensor setup for the future installation of a monitoring system. The second test (28 measuring channels) was performed between December 11th and 12th, 2017, with the objectives of obtaining a complete representation of the mode shapes and roughly assessing the impact of temperature changes on natural frequencies.

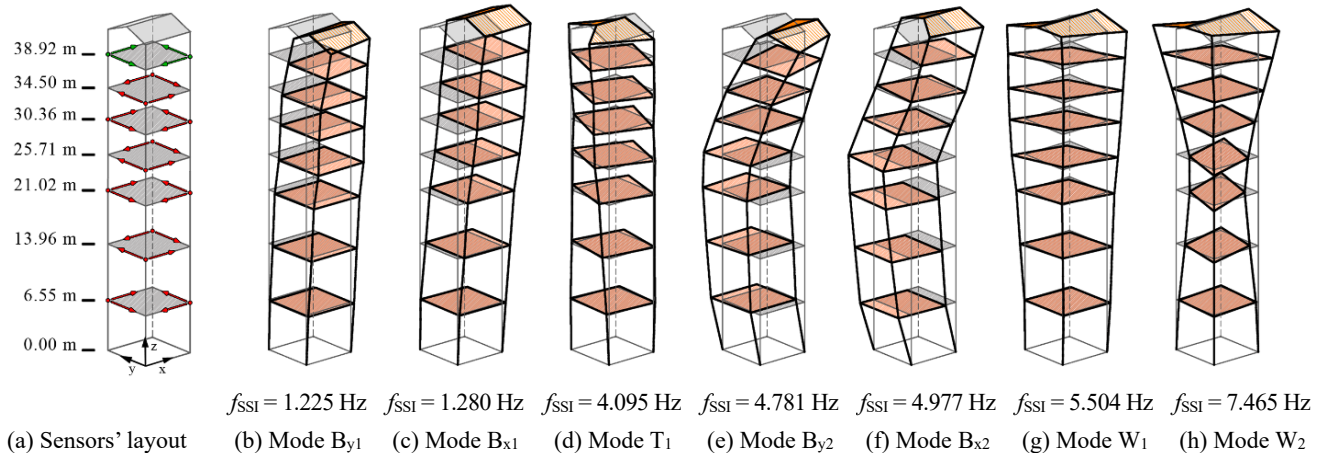


Fig. 6 Instrumented cross-sections and layout of accelerometers during the vibration test performed in December 2017, and identified vibration modes (SSI)

During the first test, 2 bi-axial seismometers (electrodynamic velocity sensors, 78 V/(m/s) sensitivity) were installed at the opposite corners of the top floor to measure the dynamic response of the structure under ambient excitation. During the second test, high-sensitivity accelerometers (sensitivity of 10 V/g; peak acceleration of ± 0.5 g) were employed to measure the response of the tower in 14 points belonging to 7 selected cross-sections (Fig. 6(a)).

The modal identification was performed using time windows of 3000 s and applying the data-driven Stochastic Subspace Identification method (SSI-data, van Overschee and de Moor 1996) available in the commercial software ARTEMIS (Structural Vibration Solutions 2012); the natural frequency estimates have also been verified through the Frequency Domain Decomposition (FDD, Brincker *et al.* 2001) algorithm.

Overall, seven vibration modes were identified in the frequency range of 0-9 Hz. The identified modes were classified as 4 bending modes (B), 1 torsion mode (T), and 2 modes involving a warping (W) distortion of the tower cross-sections. As shown in Fig. 6 (referring to the test performed on December 2017), the sequence of lower 5 modes (i.e., 2 couples of closely-spaced bending modes with an intermediate torsion mode, Figs. 6(b)-(f)) is very similar to what observed on similar towers (Cabboi *et al.* 2017, Ubertini *et al.* 2018, Standoli *et al.* 2020), whereas the last two modes (Figs. 6(g)-(h)) are distinctive features of the investigated structure. It is further noticed that, to the authors' knowledge, vibration modes involving warping distortion of the cross-sections have not been observed before on historic towers; in the case of *Zuccaro* tower, the warping distortion is conceivably related to the cross-section characteristics, namely the size of the structure's side and the absence of stiff floors.

The inspection of Fig. 6 also reveals that all identified modes are characterized by significant modal deflections of the points belonging to the upper instrumented floor: hence, those modes can be identified and correctly classified by installing 2 bi-axial sensors at the opposite corners of the top floor. This aspect, very important in view of the continuous monitoring of the structure, has been verified through the first test (October 2016). The correspondence of natural frequencies identified in the two subsequent tests is summarized in Table 1 and reveals negligible changes in the resonant frequency of the lower 6 modes, even if the air

temperature was ranging between $+10.3^{\circ}\text{C}$ and $+12.6^{\circ}\text{C}$ during the first test and between -0.1°C and $+2.0^{\circ}\text{C}$ during the second test. On the contrary, the higher mode (W_2) seems to exhibit a larger sensitivity to air temperature.

It is finally observed that the results of the test performed in December 2017 (Fig. 6) were assumed as experimental reference in the calibration of the numerical model.

4. FE modeling and updating

The 3D model of the tower was developed with the FE code ABAQUS using the eight-node brick elements (C3D8). A relatively large number of elements were employed to obtain a regular distribution of masses, a good description of the opening distribution, and to avoid frequency sensitivity to mesh size. Overall, the numerical model consists of 10,582 brick elements with 48,438 degrees of freedom and an average mesh size of 0.5 m (Fig. 7(a)).

Firstly, the geometry of the FE model is retrieved from the topographic survey. Once the geometry is established, the selection of the structural parameters to be updated is the next key issue. To prevent the ill-conditioning of the inverse problem and to improve the robustness of the parameter estimates, the number of updating variables was kept smaller than the experimental parameters used as targets (i.e., the identified natural frequencies), and only the uncertain structural parameters were updated. Consequently, the following assumptions were adopted: (a) the effect of soil-structure interaction was neglected and the tower was assumed fixed at the base; (b) the mass density and Poisson's ratio of the masonry were set equal to 17 kN/m^3 and 0.15, respectively; (c) a linear elastic orthotropic material was adopted for the brick masonry, with the shear modulus being considered equal to $G = \alpha \cdot E$, where E is the Young's modulus, and α is a constant multiplier.

As reported by Gentile *et al.* (2019b), the material properties (i.e., the Young's modulus E and the shear modulus G) of the initial model of the *Zuccaro* tower were chosen based on the results of local non-destructive tests and the recommendation of the Italian Technical Code. Furthermore, in the initial model, the connection between the tower and the neighboring buildings was neglected.

Despite the initial model represented the structural geometry accurately, the differences with the identified dynamic characteristic are substantial. As shown in Table 2, the natural frequencies of the initial model significantly differ from the experimental ones, with an average and maximum discrepancy of 11% and 21%, respectively. Moreover, the second-order bending modes (B_{x2} and B_{y2}) are reversed in order and do not follow the experimental sequence. In order to enhance the correlation between the theoretical and experimental modal response, the following aspects were considered: the presence of surrounding buildings (see, Fig. 5(a)), the in-homogeneities in the masonry walls (Fig. 5(e)), and the stiffening effect created by the timber floors (e.g., Fig. 5(c)).

Consequently (and after a sensitivity analysis), the initial model was modified by introducing the following

Table 1 Natural frequencies identified (SSI) in October 2016 and December 2017

Mode Id.	Mode type	$f_{\text{SSI-2016}}$ (Hz)	$f_{\text{SSI-2017}}$ (Hz)
B_{y1}	Bending, y-direction	1.224	1.225
B_{x1}	Bending, x-direction	1.280	1.280
T_1	Torsion	4.083	4.095
B_{y2}	Bending, y-direction	4.830	4.781
B_{x2}	Bending, x-direction	4.951	4.977
W_1	Warping distortion	5.531	5.504
W_2	Warping distortion	7.658	7.465

Table 2 Comparison between experimental frequencies ($f_{SSI-2017}$) and the corresponding frequencies of the initial (f_{FEM-I}) and optimal ($f_{FEM-OPT}$) FE model

Mode Id.	$f_{SSI-2017}$	f_{FEM-I}	DF (%)*	$f_{FEM-OPT}$	DF (%)*
B _{y1}	1.225	1.290	-5.30	1.226	-0.05
B _{x1}	1.280	1.300	-1.52	1.279	0.09
T ₁	4.095	4.434	-8.28	4.096	-0.01
B _{y2}	4.781	5.499	-15.0	4.782	-0.01
B _{x2}	4.977	5.433	-9.15	4.977	0.00
W ₁	5.504	6.684	-21.4	5.504	0.00
W ₂	7.465	8.547	-14.5	7.412	0.72

$$*DF = 100 \cdot (f_{SSI} - f_{FEM}) / f_{SSI}$$

assumptions:

- The effect of the low-rise constructions around the tower was modeled with a uniform distribution of linear elastic translational springs in the two directions – up to the height of 9.4 m – with resulting stiffness Σk_x and Σk_y ;
- The masonry walls were divided into 2 regions with constant material properties (i.e., E_{low} and E_{up}) to consider the effect of in-homogeneities in masonry walls. The height of the splitting point between the two regions was evaluated by minimizing the difference with the experimental results (Gentile *et al.* 2019b);
- The presence of timber floors was simulated with a series of rigid beams connected to the vertical walls using linear elastic springs (constant k_{TF}).

Overall, the number of updating parameters was equal to six: the Young's modulus in the lower and upper part of the building, the ratio $\alpha = G/E$ and the spring constants Σk_x , Σk_y , and k_{TF} .

Subsequently, FE model updating was performed to identify the above updating parameters. A surrogate-based procedure (Douglas and Reid 1982) was implemented in

Table 3 Lower bounds (L), optimal values (OPT) and upper bounds (U) of the structural parameters

Structural parameters	X^L	X^{OPT}	X^U
E_{low} (GPa) height \leq 21.02 m	2.68	3.08	3.62
E_{up} (GPa) height $>$ 21.02 m	1.48	1.73	2.00
A	0.315	0.335	0.349
Σk_x (kN/m $\times 10^5$)	3.43	13.73	13.75
Σk_y (kN/m $\times 10^5$)	0.001	0.001	0.011
k_{TF} (kN/m $\times 10^5$)	0.25	0.49	0.74

MATLAB: a second-order polynomial approximation neglecting the cross-terms was used as surrogate model while the minimization problem was solved with the Particle Swarm Optimization (PSO) algorithm (Kennedy and Eberhart 1995). The surrogate model was a function of the six selected parameters, and a limited number of FE analyses was required in its definition, making the use of surrogate-based model updating particularly suitable for SHM purposes.

The selected parameters were iteratively corrected in a constrained range until a minimum solution of the following objective function was found

$$J(x) = \frac{100}{n} \sum_{i=1}^n \left| \frac{f_i^{AVT} - f_i^*(x)}{f_i^{AVT}} \right| \quad (5)$$

where n is the number of natural frequencies considered, f_i^{AVT} is the i -th experimentally identified natural frequency, and $f_i^*(x)$ is the i -th polynomial approximation (Douglas and Reid 1982) of the numerical natural frequencies, expressed as functions of the x updating parameters.

Table 3 lists the optimal estimates of the uncertain structural parameters. The difference between E_{low} and E_{up} is motivated by the presence of fragmentary and non-homogeneous masonry, starting from the height of 21.02 m (Fig. 5). Moreover, the large difference between the stiffness of springs in x - and y -directions is explained by the

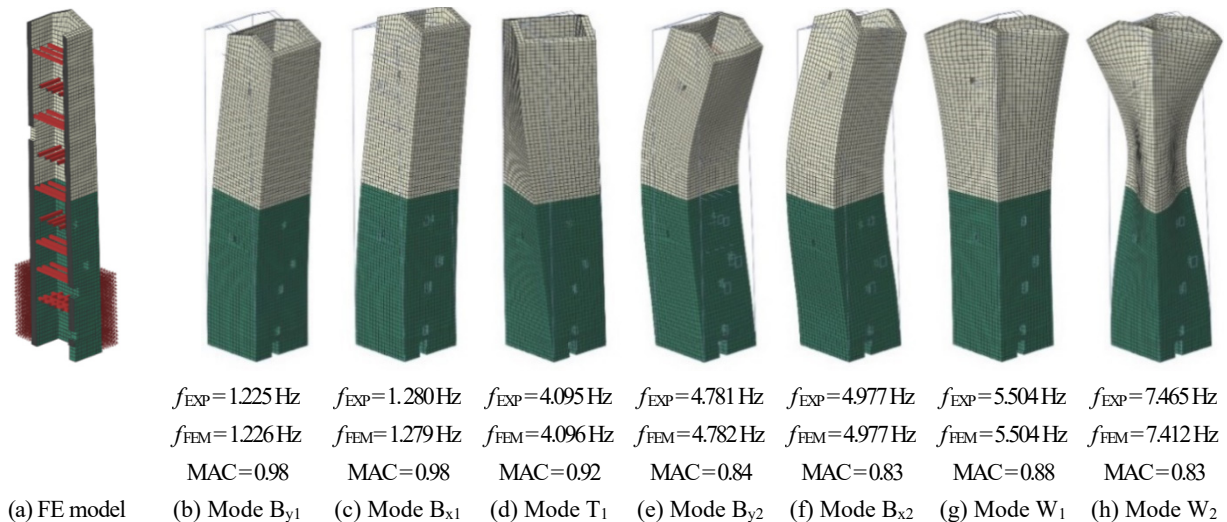


Fig. 7 FE model of the Zuccaro tower and vibration modes of the optimal (updated) model

geometry of the surrounding constructions. In x-direction, the constraint effect is given by a building aggregate, while in the y-direction, just an isolated block of limited dimension is present.

Fig. 7 shows the mode shapes of the optimal (updated) model, corresponding to the experimental ones (Fig. 6), and the correlation with the modal parameter of the real building. It should be noticed that an excellent correlation between the numerical and experimental modal responses is obtained, resulting in a maximum frequency discrepancy of 0.71% and a minimum MAC (Allemang and Brown 1982) of 0.83. Hence, the optimal model is capable of accurately representing the observed dynamic characteristics of the building and can be considered an appropriate baseline model for long-term dynamic monitoring.

5. Application of the DLRM approach

As previously pointed out, to test the proposed damage identification methodology, different damage scenarios (DS) were simulated on the pseudo-experimental monitoring data of the *Zuccaro* tower.

The frequency data are generated based on the assumption that the structural response is affected only by the temperature changes. Therefore, the optimized FE model and the collected external temperatures were used to generate the variations of natural frequencies over three years. Subsequently, the environmental effects were removed using PCA-based regression, and the damage identification was performed with the proposed DLRM approach (Fig. 1). The damage scenarios are assumed as permanent shifts on the natural frequencies, affecting only the stiffness of small portions of the masonry walls.

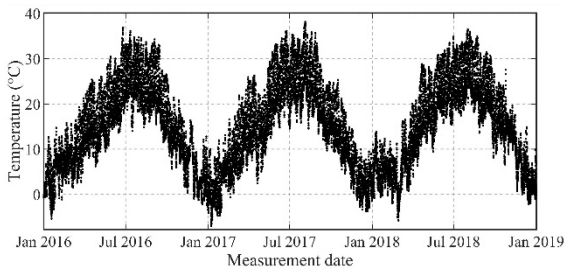
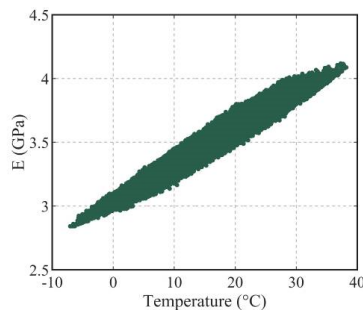
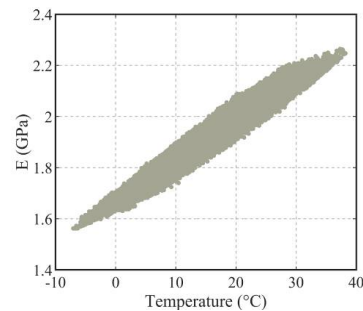


Fig. 8 Temperature data from S. Agnese weather station (from January 2016 to December 2018)



(a) E_{low} height ≤ 21.02 m



(b) E_{up} height > 21.02 m

Fig. 9 Correlation between the air temperature and the Young's modulus of lower and upper parts of the tower

5.1 Pseudo-experimental frequency data

Firstly, an empirical relationship between the temperature and the Young's modulus of the brick masonry was developed. To this purpose, the frequency-temperature data previously obtained on the *Gabbia* tower (Gentile *et al.* 2016) were considered: it is worth mentioning that the *Gabbia* tower is an ancient masonry building located 200 m far from the *Zuccaro* tower, with similar geometry and construction materials.

In more details, it has been assumed that the i -th Young's modulus $E_{i,k}$ at time k depends on the temperature at the same instant k and the temperature of the previous 6 and 12 hours

$$g(T_k) = \frac{0.1 \cdot E_i^{AVT}}{10^\circ C} \cdot (T_k - T^{AVT}) \quad (6)$$

$$\begin{aligned} E_{i,k}(T_k, T_{k-6h}, T_{k-12h}) \\ = 0.6 \cdot g(T_k) + 0.3 \cdot g(T_{k-6h}) \\ + 0.1 \cdot g(T_{k-12h}) + E_i^{AVT} \end{aligned} \quad (7)$$

where E_i^{AVT} is the i -th Young's modulus identified with the model updating procedure from the AVT data and T^{AVT} is the average temperature during the AVT.

The temperature data (Fig. 8) between January 2016 and December 2018 were retrieved from the S. Agnese weather station of the Local Environmental Agency (ARPA Lombardia), which is about 300 m far from the investigated structure. Subsequently, the empirical relationships Eqs. (5)-(6) were used to generate the variations of the Young's modulus on the optimal model (Fig. 9) and to obtain the corresponding frequency data (Fig. 10(a)). Furthermore, to simulate the presence of noise on the generated data, a normal distribution with a pre-defined standard deviation was assumed for each frequency (Table 4 and Fig. 10(b)). The level of noise was calibrated from similar studies (Gentile *et al.* 2016, Cabboi *et al.* 2017), considering the standard deviations of the identified frequencies before and after the removal of environmental effects.

As stated in Section 2, the adopted damage detection strategy employs cleansed frequency data. Consequently, the fluctuations caused by environmental effects are removed with a PCA-based regression using a training period of 12 months (Fig. 11). The regression model is used to predict the modal frequencies after the training period, possibly revealing the presence of structural anomalies. The

Table 4 Statistics of the pseudo-experimental frequency data with 3 simulated damage scenarios

Mode Id.	Added noise	Pseudo-experimental data		Filtered data	Damage Scenarios (DS)		
	σ_f (Hz)	f (Hz)	σ_f (Hz)	σ_f (Hz)	Δf_{DS1} (Hz)	Δf_{DS2} (Hz)	Δf_{DS3} (Hz)
B _{y1}	0.005	1.297	0.052	0.005	0.006	0.001	0.000
B _{x1}	0.005	1.350	0.051	0.005	0.001	0.001	0.000
T ₁	0.008	4.333	0.169	0.009	0.010	0.008	0.000
B _{y2}	0.010	5.062	0.200	0.011	0.006	0.002	0.001
B _{x2}	0.012	5.248	0.194	0.012	0.007	0.012	0.001
W ₁	0.020	5.773	0.193	0.018	0.000	0.001	0.012
W ₂	0.030	7.799	0.279	0.027	0.001	0.010	0.004

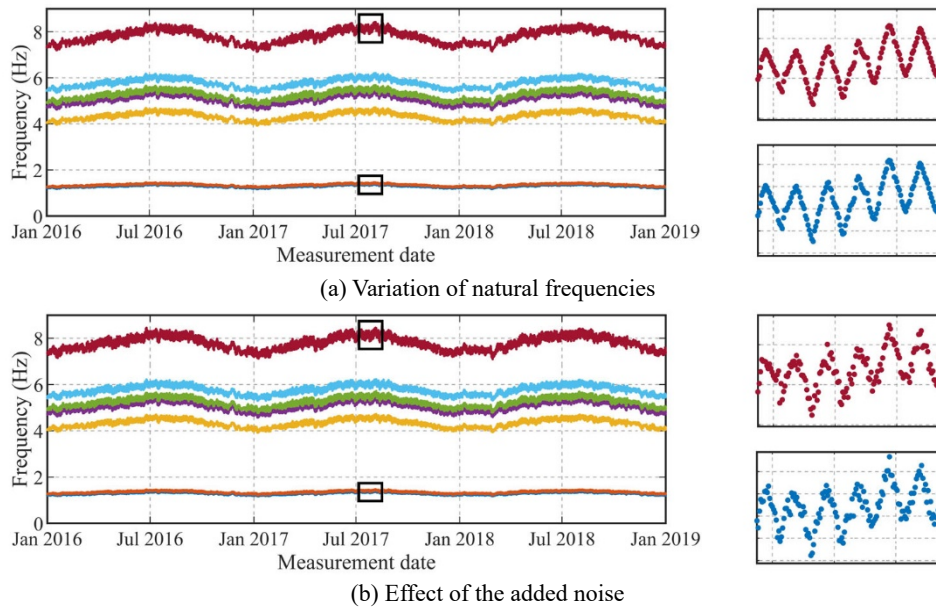


Fig. 10 Three years of pseudo-experimental data and 6-days zooms of the first (B_{y1}) and last (W₂) mode

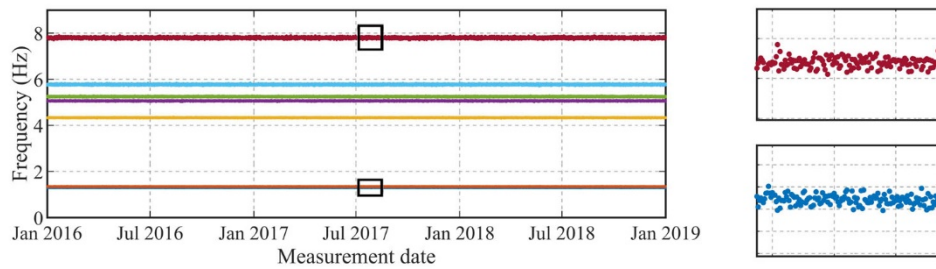


Fig. 11 Filtered data from PCA-based regression: variations over three years and 6-days zooms of the first (B_{y1}) and last (W₂) frequency

comparison of Fig. 10(b) and Fig. 11 demonstrates the effectiveness of the adopted procedure in cleaning the data. It is worth noting that the resulting standard deviation after the filtering corresponds almost completely with the added noise (Table 4).

5.2 Simulation of damage scenarios

Once the frequency time series were generated, three DSs were simulated using the optimal FE model. Fig. 12(a) shows the selected elements, which belong to different

regions of the tower: lower (DS1), medium (DS2), and upper (DS3) part. In more details:

- DS1 corresponds to 20% decrease in the Young's modulus of a masonry wall at the ground floor and induces a maximum frequency decrease of about 1% in the first mode (B_{y1});
- DS2 corresponds to 30% decrease in the Young's modulus of a masonry portion at the fifth floor, involving a maximum frequency reduction of about 0.8% in the fifth mode (B_{x2});

- DS3 corresponds to 30% decrease in the Young’s modulus of a masonry wall at the top floor, generating a maximum frequency shift of about 0.7% in the sixth mode (W_1).

DS1 and DS3 were simulated during the winter season (1st of February) – when the daily frequency variations are smaller – while DS2 was simulated during the summer season (1st of July). Subsequently, the random noise was added on the generated data, hiding the sharp changes of natural frequencies in the daily variations caused by environmental effects; it is indeed impossible to recognize the frequency shifts inspecting the diagram (Fig. 12(d)).

Table 4 illustrates the adopted mean values and standard deviations for the pseudo-experimental monitoring data and reports the effects of the three DSs on the 7 natural frequencies considered. It is worth noting that the DSs have comparable frequency shifts than the standard deviations after the filtering.

5.3 Vibration-based damage detection and localization

Firstly, novelty analysis was applied to detect the presence of anomalies on the data. Subsequently, the anomalies are localized using the DLRM approach, comparing the detected frequency shifts with the ones numerically computed.

The residual errors obtained from the PCA-based regression were used to define a multivariate control chart based on the Hotelling’s T^2 -statistic. The data were divided into subgroups of 12 hours, and a process mean was defined using a period of 12 months. The structural anomalies are detected each time an observation lays outside the control limit. As shown in Fig. 13(a), the three damage scenarios are clearly detected, and more specifically:

- During the training period a limited number of observations exceed the control limit;
- At the time the damage is introduced, the control limit is suddenly exceeded by the T^2 -statistic, exhibiting a more significant dispersion.

Once the presence of a structural anomaly is detected, the localization is performed with the DLRM approach (Figs. 13(b)-(c)). The damage location matrix was created employing the previously updated numerical model. The model was divided into 80 elements – 8 elements per floor – to capture the possible effect of local damages. The Young’s modulus of each element is decreased by 50%, and the resulting frequency shifts are collected as described in Section 2. Nevertheless, due to the approximate symmetry of the structure, it is not expected to distinguish between damages occurring in parallel walls.

The comparison between the pseudo-experimental frequency shifts and the computed DLRM is performed by

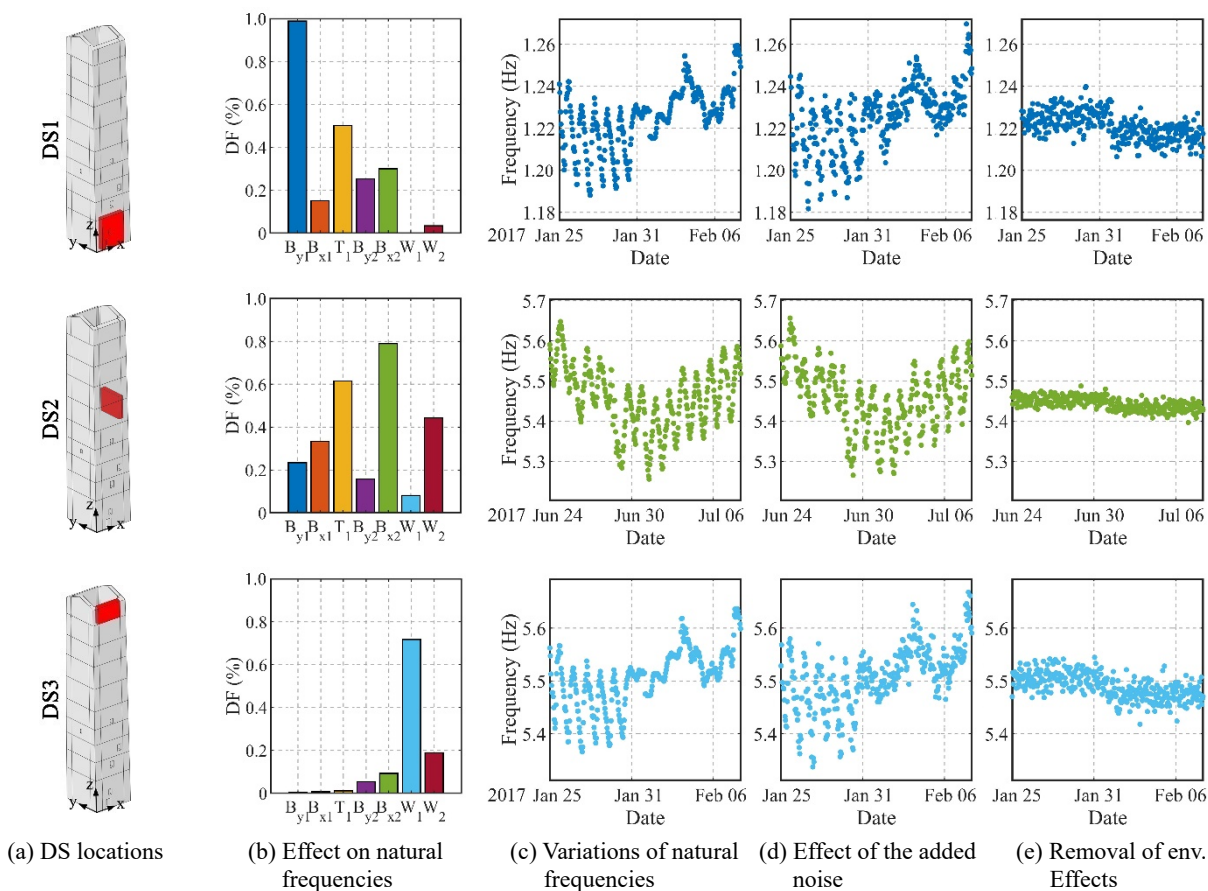


Fig. 12 Simulated damage scenarios (DSs): actual locations, percentage variation of natural frequencies and 12-days zooms of the natural frequencies most affected by damage

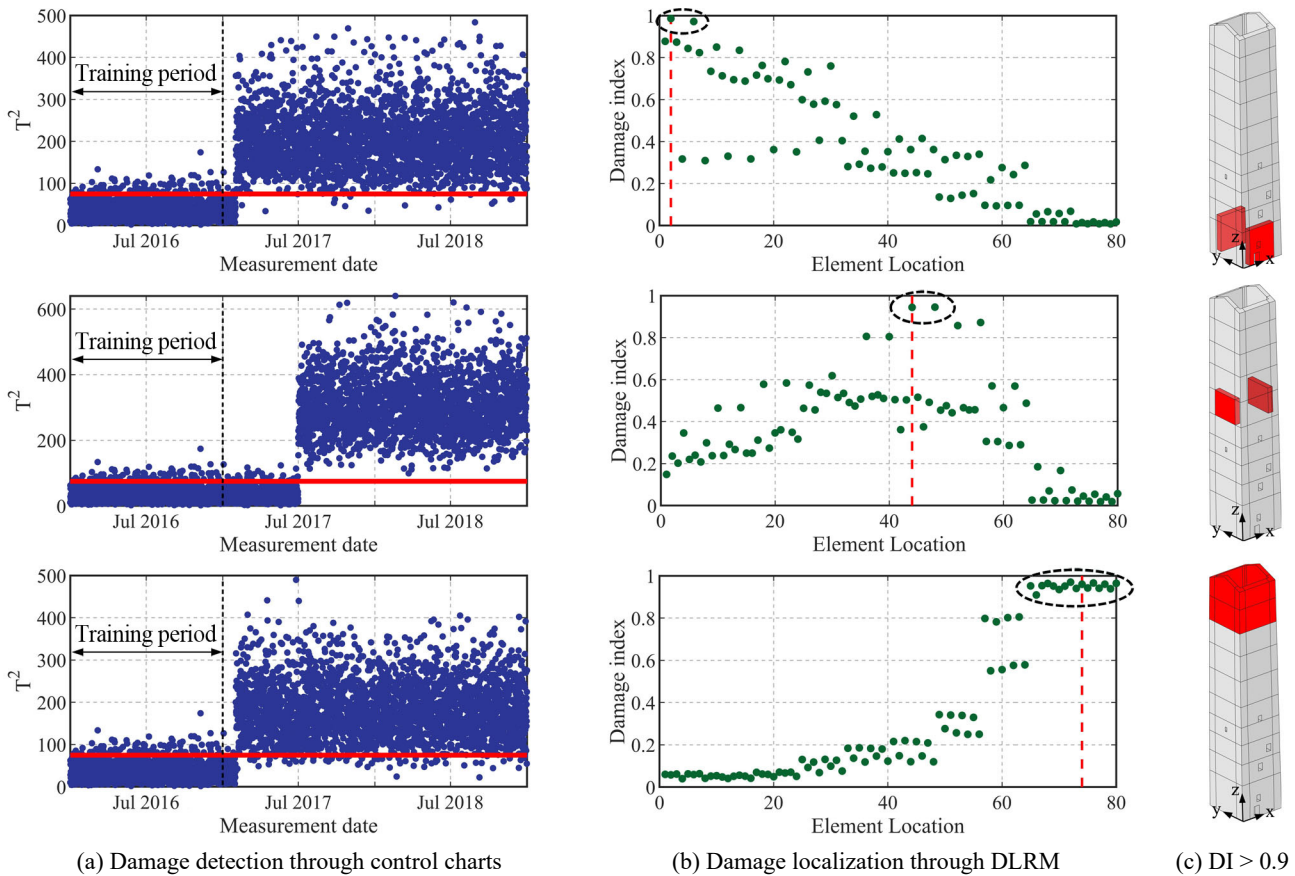


Fig. 13 Damage detection and localization for the three simulated damages

using Eq. (4). The results just after the damage detection from the control charts are shown in Fig. 13(b). The red dashed line represents the correct damage location, whereas the green dots are the Damage Indexes (DIs) of each element. The elements with higher DIs are more likely to be damaged. The localization is more precise for DS1 and DS2, while the algorithm is less effective for DS3. Fig. 13(c) illustrate the positions of the elements with a Damage index higher than 0.90. The inspection of Fig. 13 suggests the following comments:

- The DS1 is correctly localized in the lower part of the tower on the walls along the x-direction;
- Similarly, the DS2 is correctly localized between the 5th and 6th floors on the walls along the y-direction;
- The DS3 is correctly localized in the top floor of the tower, but it was not possible to distinguish on which wall.

Notably, the localization of the last DS relies on the induced frequency shift on mode W_1 (see Fig. 12(b), DS3), which is associated with distortion of the cross-section. Conversely, the other localizations rely also on bending modes (see Fig. 12(b), DS1 and DS2), which are characterized by a direction-dominated component of motion. As a consequence, when the damage affects mainly the warping modes its localization through the DLRM approach turns out to be less accurate even if the region involved is roughly identified.

6. Conclusions

Prior research has demonstrated the effectiveness of damage localization for masonry towers using monitored frequency data and FE modeling (Cabboi *et al.* 2017, Venanzi *et al.* 2020). In this study, further investigations are carried out to increase the capability of accurate real-time damage assessment, enhancing the resolution of the damage localization. Accordingly, a model-based damage identification procedure – named DLRM – based on computed damage scenarios is illustrated. Finally, the proposed procedure is exemplified on the *Zuccaro* tower, an ancient masonry structure built in the Middle Ages in the city of Mantua, Italy.

The damage identification methodology is based on the following steps:

- (1) The development of a FE model that accurately represents the information collected on-site, namely the structural geometry, the material inhomogeneities, and the modal parameters identified from the operational modal analysis. To this purpose, FE model updating is used to enhance the correlation with the experimental dynamic behavior.
- (2) The installation of a monitoring system consisting of a few sensors placed at the top of the building is required. Subsequently, the identification and tracking of natural frequencies are performed with

state-of-the-art techniques; thus, regression analysis – such as the PCA – is applied to filter the daily and seasonal variations caused by environmental effects.

- (3) The detection is performed using the residuals from the regression analysis through the control charts. At the same time, the localization is carried out comparing the detected experimental frequencies shift, and the numerically computed frequencies shifts, collected in the DLRM.

In summary, the overall results from the application of the methodology suggest the following conclusions:

- In masonry towers, and generally in slender structures, the mutual variation of natural frequencies caused by a structural damage is directly correlated with the damage location, making possible the localization using only frequency data;
- A cost-effective monitoring setup composed by few sensors can be used not only to detect but also to localize a structural damage.

Regarding the specific results on the *Zuccaro* tower, the simulated frequency shifts added to the pseudo-experimental monitoring data were detected and localized with the proposed approach, suggesting the future application of the methodology for the SHM of the building. To expand the capability of the proposed approach, further investigations with multiple damage scenarios should be performed.

Acknowledgments

Sincere thanks are due to M. Cucchi (LPMSC, Politecnico di Milano) and A. Ruccolo (Ph.D. candidate, Politecnico di Milano), who assisted the authors in conducting the field tests.

References

- Allemang, R.J. and Brown, D.L. (1982), “Correlation coefficient for modal vector analysis”, *Proceedings of the 1st International Modal Analysis Conference*, Orlando, FL, USA.
- Azzara, R.M., De Roeck, G., Girardi, M., Padovani, C., Pellegrini, D. and Reynders, E. (2018), “The influence of environmental parameters on the dynamic behaviour of the San Frediano bell tower in Lucca”, *Eng. Struct.*, **156**, 175-187. <https://doi.org/10.1016/j.engstruct.2017.10.045>
- Bartoli, G., Betti, M. and Vignoli, A. (2016), “A numerical study on seismic risk assessment of historic masonry towers: a case study in San Gimignano”, *Bull. Earthq. Eng.*, **14**(6), 1475-1518. <https://doi.org/10.1007/s10518-016-9892-9>
- Bellino, A., Fasana, A., Garibaldi, L. and Marchesiello, S. (2010), “PCA-based detection of damage in time-varying systems”, *Mech. Syst. Signal Process.*, **24**(7), 2250-2260. <https://doi.org/10.1016/j.ymsp.2010.04.009>
- Binda, L., Gatti, G., Mangano, G., Poggi, C. and Sacchi Landriani, G. (1992), “The collapse of the Civic Tower of Pavia: a survey of the materials and structure”, *Masonry Int.*, **20**(6), 11-20.
- Binda, L., Tongini Folli, R. and Mirabella Roberti, G. (2000), “Survey and investigations for the diagnosis of damage in masonry structures: the ‘‘Torrazzo’’ of Cremona”, *Proceedings of the 12th International Brick/Block Masonry Conference*, Madrid, Spain, June.
- Brincker, R., Zhang, L. and Andersen, P. (2001), “Modal identification of output-only systems using frequency domain decomposition”, *Smart Mater. Struct.*, **10**(3), 441-445. <https://doi.org/10.1088/0964-1726/10/3/303>
- Caboi, A., Gentile, C. and Saisi, A. (2017), “From continuous vibration monitoring to FEM-based damage assessment: application on a stone-masonry tower”, *Constr. Build. Mater.*, **156**, 252-265. <https://doi.org/10.1016/j.conbuildmat.2017.08.160>
- Cantieni, R. (2014), “One-year monitoring of a historic bell tower”, *Proceedings of the 9th International Conference on Structural Dynamics, EURO DYN 2014*, Porto, Portugal, January.
- Diaferio, M., Foti, D. and Sepe, V. (2007), “Dynamic identification of the tower of the Provincial Administration Building, Bari, Italy”, *Proceedings of the 11th International Conference on Civil, Structural and Environmental Engineering Computing*, Malta, September.
- Diaferio, M., Foti, D. and Potenza, F. (2018), “Prediction of the fundamental frequencies and modal shapes of historic masonry towers by empirical equations based on experimental data”, *Eng. Struct.*, **156**, 433-442. <https://doi.org/10.1016/j.engstruct.2017.11.061>
- Doebbling, S.W., Farrar, C.R. and Prime, M.B. (1998), “A summary review of vibration-based damage identification methods”, *Shock Vib. Digest*, **30**(2), 91-105.
- Douglas, B.M. and Reid, W.H. (1982), “Dynamic tests and system identification of bridges”, *J. Struct. Div. ASCE*, **108**(10), 2295-2312.
- Elyamani, A., Caselles, O., Roca, P. and Clapes, J. (2017), “Dynamic investigation of a large historical cathedral”, *Struct. Control Health Monitor.*, **24**(3), e1885. <https://doi.org/10.1002/stc.1885>
- Gentile, C. and Saisi, A. (2007), “Ambient vibration testing of historic masonry towers for structural identification and damage assessment”, *Constr. Build. Mater.*, **21**(6), 1311-1321. <https://doi.org/10.1016/j.conbuildmat.2006.01.007>
- Gentile, C., Guidobaldi, M. and Saisi, A. (2016), “One-year dynamic monitoring of a historic tower: damage detection under changing environment”, *Meccanica*, **51**(11), 2873-2889. <https://doi.org/10.1007/s11012-016-0482-3>
- Gentile, C., Ruccolo, A. and Canali, F. (2019a), “Long-term monitoring for the condition-based structural maintenance of the Milan Cathedral”, *Constr. Build. Mater.*, **228**, 117101. <https://doi.org/10.1016/j.conbuildmat.2019.117101>
- Gentile, C., Saisi, A. and Borlenghi, P. (2019b), “FE modelling for seismic assessment of an ancient tower from ambient vibration survey”, *Proceedings of the 8th IOMAC - International Operational Modal Analysis Conference*, Copenhagen, Denmark, May.
- Hotelling, H. (1947), “Multivariate quality control-illustrated by the air testing of sample bombsights”, in Eisenhart C. et al. (ed.) *In: Techniques of Statistical Analysis*, pp. 111-184.
- ISMES (1990), “Indagine conoscitiva e monitoraggio delle strutture murarie e del terreno di fondazione della torre degli Zuccaro (MN)”, Technical Report. [In Italian]
- Jolliffe, I.T. (2002), *Principal Component Analysis*, Springer, New York, NY, USA.
- Kennedy, J. and Eberhart, R. (1995), “Particle Swarm Optimization”, *Proceedings of IEEE International Conference on Neural Networks, Perth, Australia*, November.
- Kim, J.T. and Stubbs, N. (2003), “Crack detection in beam-type structures using frequency data”, *J. Sound Vib.*, **259**(1), 145-160. <https://doi.org/10.1006/jsvi.2002.5132>

- Kita, A., Cavalagli, N. and Ubertini, F. (2019), "Temperature effects on static and dynamic behavior of Consoli Palace in Gubbio, Italy", *Mech. Syst. Signal Process.*, **120**, 180-202. <https://doi.org/10.1016/j.ymssp.2018.10.021>
- Lionello, A., Cavaggioni, I., Modena, C., Casarin, F., Rossi, P.P. and Rossi, C. (2004), "Experimental and numerical analysis of the structural behaviour of St. Stefano's bell-tower in Venice", *Proceedings of the 4th International Seminar on Structural Analysis of Historic Constructions*, Padova, Italy, November.
- Lorenzoni, F., Casarin, F., Modena, C., Caldon, M., Islami, K. and da Porto, F. (2013), "Structural health monitoring of the Roman Arena of Verona, Italy", *J. Civil Struct. Health Monitor.*, **3**(4), 227-246. <https://doi.org/10.1007/s13349-013-0065-0>
- Masciotta, M.-G., Roque, J.C.A., Ramos, L.F., Lourenço, P.B. (2016), "A multidisciplinary approach to assess the health state of heritage structures: the case study of the Church of Monastery of Jerónimos in Lisbon", *Constr. Build. Mater.*, **116**, 169-187. <https://doi.org/10.1016/j.conbuildmat.2016.04.146>
- Messina, A., Williams, E.J. and Contursi, T. (1998), "Structural damage detection by a sensitivity and statistical-based method", *J. Sound Vib.*, **216**(5), 791-808. <https://doi.org/10.1006/jsvi.1998.1728>
- Milani, G. and Clementi, F. (2019), "Advanced seismic assessment of four masonry bell towers in Italy after operation modal analysis (OMA) identification", *Int. J. Arch. Herit.*, [In press] <https://doi.org/10.1080/15583058.2019.1697768>
- Montgomery, D.C. (1997), *Introduction to Statistical Quality Control*, John Wiley & Sons, New York, NY, USA.
- Peña, F., Lourenço, P.B., Mendes, N. and Oliveira, D.V. (2010), "Numerical models for the seismic assessment of an old masonry tower", *Eng. Struct.*, **32**(5), 1466-1478. <https://doi.org/10.1016/j.engstruct.2010.01.027>
- Potenza, F., Federici, F., Lepidi, M., Gattulli, V., Graziosi, F. and Colarieti, A. (2015), "Long-term structural monitoring of the damaged Basilica S. Maria di Collemaggio through a low-cost wireless sensor network", *J. Civil Struct. Health Monitor.*, **5**(5), 655-676. <https://doi.org/10.1007/s13349-015-0146-3>
- Ramos, L.F., Aguilar, R., Lourenço, P.B. and Moreira, S. (2013), "Dynamic structural health monitoring of Saint Torcato church", *Mech. Syst. Signal Process.*, **35**(1-2), 1-15. <https://doi.org/10.1016/j.ymssp.2012.09.007>
- Saisi, A., Terenzoni, S., Ruccolo, A. and Gentile, C. (2019), "Safety of the architectural heritage: structural assessment of the Zuccaro's tower in Mantua", in Aguilar R. et al. (ed.), In: *Structural Analysis of Historical Constructions*, RILEM Bookseries, **18**, 2422-2430. https://doi.org/10.1007/978-3-319-99441-3_260
- Standoli, G., Giordano, E., Milani, G. and Clementi, F. (2020), "Model updating of historical belfries based on OMA identification techniques", *Int. J. Archit. Herit.*, [In press] <https://doi.org/10.1080/15583058.2020.1723735>
- Structural Vibration Solutions (2012), ARTeMIS Extractor Pro 2011, Aalborg, Denmark.
- Ubertini, F., Cavalagli, N., Kita, A. and Comanducci, G. (2018), "Assessment of a monumental masonry bell-tower after 2016 central Italy seismic sequence by long-term SHM", *Bull. Earthquake Eng.*, **16**(2), 775-801. <https://doi.org/10.1007/s10518-017-0222-7>
- Valente, M. and Milani, G. (2016), "Seismic assessment of historical masonry towers by means of simplified approaches and standard FEM", *Constr. Build. Mater.*, **108**, 74-104. <https://doi.org/10.1016/j.conbuildmat.2016.01.025>
- van Overschee, P. and de Moor, B. (1996), *Subspace Identification for Linear Systems: Theory, Implementation, Applications*, Kluwer Academic Publishers, Dordrecht, The Netherlands.
- Venanzi, I., Kita, A., Cavalagli, N., Ierimonti, L. and Ubertini, F. (2020), "Earthquake-induced damage localization in an historic masonry tower through long-term dynamic monitoring and FE model calibration", *Bull. Earthq. Eng.*, **18**(5), 2247-2274. <https://doi.org/10.1007/s10518-019-00780-4>
- Yan, A.-M., Kerschen, G., De Boe, P. and Golinval, J.-C. (2005), "Structural damage diagnosis under varying environmental conditions - Part I: A linear analysis", *Mech. Syst. Signal Process.*, **19**(4), 847-864. <https://doi.org/10.1016/j.ymssp.2004.12.002>
- Zonno, G., Aguilar, R., Boroschek, R. and Lourenço, P.B. (2019), "Analysis of the long and short-term effects of temperature and humidity on the structural properties of adobe buildings using continuous monitoring", *Eng. Struct.*, **196**, 109299. <https://doi.org/10.1016/j.engstruct.2019.109299>